

## Identified Particle Production in p+p, d+Au, and Au+Au Collisions at RHIC

Felix Matathias<sup>1</sup> for the PHENIX Collaboration

<sup>1</sup> Columbia University, Nevis Laboratories,  
PO Box 137, Irvington, NY 10533, U.S.A.

**Abstract.** Measurements of identified particle production with the PHENIX experiment at RHIC have reached a mature state, where a multitude of nuclear systems at different colliding energies have been studied. The discovery configurations of  $\sqrt{s_{NN}} = 130$  and 200 GeV Au+Au collisions have now been supplemented by additional Au+Au and Cu+Cu configurations at various energies, along with baseline p+p and d+Au runs at  $\sqrt{s_{NN}} = 200$  GeV. In this work we present a systematic study of the Cronin effect in d+Au collisions and recent results from p+p collisions. We then proceed to make a critical comparison of pion, kaon and proton production in heavy ion and baseline systems, and discuss the observed nuclear effects on hadron production.

*Keywords:* RHIC, PHENIX, QGP, pQCD, Cronin, Au+Au, d+Au, p+p  
*PACS:* 12.38.Mh, 12.38.-t, 13.85.-t, 13.85.Ni, 14.20.Dh, 14.40.Aq, 24.85.+p, 25.75.Nq, 25.75.-q, 25.75.Dw

### 1. Introduction

The abundance and composition of particles that reached the PHENIX detectors after central collisions of Au nuclei at  $\sqrt{s_{NN}} = 130$  and 200 GeV generated a lot of excitement in the Relativistic Heavy Ion community soon after the Relativistic Heavy Ion Collider (RHIC) assumed operations. The transverse momentum spectra of pions were greatly suppressed by factors of 4-5 at high  $p_T$  [ 1, 2] compared to expectations from point-like scaling, and the proton and antiproton  $p_T$  spectra, in contrast to any expectation or prediction, crossed the pionic spectra at around 2 GeV in  $p_T$  [ 3, 4, 5]. For the first time, matter created in the laboratory had reached such exotic conditions of temperature and pressure that the creation of a pion or a proton were equally probable, despite their mass difference and quark content. Suppression of high energetic particles had been long expected to be the smoking gun signature of the creation of Quark Gluon Plasma [ 6, 7], where hard-scattered

partons suffer energy loss as they propagate through the hot and dense medium. The particle composition anomaly though was a complete surprise and to this day constitutes one of the great discoveries of the relativistic heavy ion programme at PHENIX, and RHIC in general.

Many theoretical works assumed the task of explaining these remarkable properties of super-heated partonic matter and we now have a much firmer theoretical understanding of the underlying dynamics of heavy ion collisions at RHIC energies, but due to the hugely successful performance of the RHIC collider in the next 4 years after the first discoveries, the wealth of experimental data are still at the forefront of the community's efforts to solve the Quark Gluon Plasma puzzle. With the successful completion of the fifth year of RHIC operations in 2005, which provided Cu+Cu collisions and polarized p+p collisions, PHENIX has recorded data on Au+Au collisions at  $\sqrt{s_{NN}} = 19.6, 62.4, 130,$  and  $200$  GeV, Cu+Cu collisions at  $\sqrt{s_{NN}} = 22.5, 62.4,$  and  $200$  GeV, along with baseline measurements in p+p and d+Au collisions at  $\sqrt{s_{NN}} = 200$  GeV.

The novel effects observed in central Au+Au collisions require a detailed account of the initial state conditions. The effects from the initial state are best studied by performing a control experiment in which only cold nuclear matter is produced. Deuteron + gold collisions at  $\sqrt{s_{NN}} = 200$  GeV serve this purpose. Since hot and dense final state medium is not created in these type of collisions, the initial state conditions become accessible to the experiment. Known initial state effects include nuclear shadowing and gluon saturation [ 8], along with the Cronin effect [ 9, 10, 11], which enhances the hadron yields, and, therefore, acts in the opposite direction compared to the suppression of particle yields in central Au+Au collisions. The Cronin effect is usually attributed to momentum broadening due to multiple initial state scattering [ 12, 13, 14, 15, 16, 17] but the species dependence of the effect is not yet completely understood and further experimental study is interesting in its own right. Since it has been observed that at lower energies, Cronin enhancement is stronger for protons than for pions [ 11], this effect has to be considered at RHIC energies before new physics for baryon and meson production is invoked.

Recently, Hwa and collaborators provided an alternative explanation due to final state interactions. The particle species dependent enhancement is attributed to recombination of shower quarks with those from the medium, where no distinction is made if hot or cold nuclear matter is produced [ 18]. Identified hadron production measured as a function of centrality brings important experimental handles to this long outstanding problem. The dependence of the enhancement upon the thickness of the medium can differentiate among the scattering models, and the species dependence helps to separate initial from final state effects in d+Au.

## 2. Experiment and Data Analysis

Data presented here include collisions at  $\sqrt{s_{NN}} = 200$  GeV of Au+Au taken in the 2002 run of RHIC, and d+Au and p+p collected in 2003. In the following we

discuss analysis of the p+p and d+Au data; details of the Au+Au analysis are found in [ 5]. Events with vertex position along the beam axis within  $|z| < 30$  cm were triggered by the Beam-Beam Counters (BBC) located at  $|\eta| = 3.0-3.9$  [ 19]. The minimum bias trigger accepts  $88.5 \pm 4\%$  of all d+Au collisions that satisfy the vertex condition, and  $51.6 \pm 9.8\%$  of p+p collisions. A total of  $42 \times 10^6$  d+Au events and  $25 \times 10^6$  minimum bias p+p events were analyzed.

In p+p collisions, differential invariant cross section is calculated by Eq. 1

$$E \frac{d^3\sigma}{dp^3} = \frac{\sigma_{BBC}}{N_{BBC}^{Total}} \cdot \frac{1}{2\pi} \cdot \frac{1}{p_T} \cdot C_{eff}^{geo}(p_T) \cdot \frac{1}{C_{bias}^{BBC}} \cdot \frac{d^2N}{dp_T dy} \quad (1)$$

The BBC trigger cross section,  $\sigma_{BBC}$ , was determined via the van der Meer scan technique and it was measured to be  $\sigma_{BBC} = 23 \pm 2.1(9.6\%)$  mb. The factor  $C_{eff}^{geo}(p_T)$  denotes the efficiency and geometrical acceptance correction, calculated with a detailed GEANT Monte Carlo simulation of the PHENIX aperture.  $C_{eff}^{geo}(p_T)$  normalizes the cross section in one unit of rapidity and full azimuthal coverage. The  $C_{bias}^{BBC}$  factor corrects for the fact that the forward BBC trigger counters see only a fraction of the inelastic p+p cross section. This subset of events that the BBC triggers on, contains only a fraction of the inclusive particle yield at mid-rapidity. For charged hadrons this factor was determined to be  $0.80 \pm 0.02$ , independent of  $p_T$ , using the data from the beam bunch crossing triggers.

There were no van der Meer scans performed during the d+Au run, and therefore PHENIX only measures the inelastic yield per BBC triggered event. The collision centrality is selected in d+Au using the south (Au-going side) BBC (BBCS). We assume that the BBCS signal is proportional to the number of participating nucleons ( $N_{part}^{Au}$ ) in the Au nucleus, and that the hits in the BBCS are uncorrelated to each other. Using a Glauber model [ 20] and simulation of the BBC, we define 4 centrality classes in d+Au collisions, as was discussed in detail in [ 21]. The mean number of binary collisions that correspond to each centrality bin are  $15.4 \pm 1.0$ ,  $10.6 \pm 0.7$ ,  $7.0 \pm 0.6$  and  $3.1 \pm 0.3$  for the most peripheral d+Au bin. For the Minimum Bias d+Au collisions  $\langle N_{coll} \rangle = 8.5 \pm 0.4$ .

Charged particles are reconstructed using a drift chamber (DC) and two layers of multi-wire proportional chambers with pad readout (PC1, PC3) [ 19]. Particle identification is based on particle mass calculated from the measured momentum and the velocity obtained from the time-of-flight and path length along the trajectory. The measurement uses the portion of the east arm spectrometer containing the high resolution time-of-flight (TOF) detector, which covers pseudo-rapidity  $|\eta| = 0.35$  and  $\Delta\phi = \pi/8$  in azimuthal angle. The timing uses the BBC for the global start, and stop signals from the TOF scintillators located at a radial distance of 5.06 m. The system resolution is  $\sigma \approx 130$  ps.

Corrections to the charged particle spectrum for geometrical acceptance, decays in flight, reconstruction efficiency, energy loss in detector material, and momentum resolution are determined using a single-particle GEANT Monte Carlo simulation. The proton and antiproton spectra are corrected for feed-down from weak decays using a Monte Carlo simulation which uses experimental data as input for particle

composition and the  $\Lambda$  spectrum from [ 22], [ 23], [ 24], [ 25], [ 26]. The Monte Carlo is used to decay and propagate the products of the weak decays through the PHENIX magnetic field and central arm detectors. The resulting feed-down proton and antiproton spectra are then subtracted from the inclusive measured spectra. The contribution from feed-down protons is approximately 30% at moderate and high  $p_T$  increasing slowly to 40% at  $p_T = 0.6$  GeV/c.

### 2.1. Systematic Uncertainties

Systematic uncertainties on the hadron spectra arise from the small remaining contamination by other species, backgrounds remaining after the matching hit requirement in the TOF, and residual time variations in the TOF timing. Uncertainties due to particle identification cuts are momentum dependent. For protons and antiprotons, the identification uncertainty is 8% at low  $p_T$  and decreases to 3% at high  $p_T$ . Kaons at low momentum have 10% PID uncertainty, decreasing to 3% at high  $p_T$ . For pions the uncertainty increases from 4 to 10 % with increasing  $p_T$ . The systematic error on the feed-down proton spectrum is 24%, primarily due to uncertainty in the measured  $\Lambda$  spectra and particle composition. The resulting systematic error on the final prompt proton and antiproton spectra is of the order of 10% in both p+p and d+Au. The systematic error on the proton to pion ratio is 12%, including the uncertainty on  $\bar{\Lambda}/\Lambda$ .

Systematic uncertainties on the d+Au nuclear modification factors mostly cancel as the p+p and d+Au data were collected immediately following one another, and detector performance was very similar. The overall systematic error in the nuclear modification factor is due to uncertainties in the reconstruction efficiencies, fiducial volumes, and small run-by-run variations. It is approximately 10%, independent of  $p_T$ . An additional d+Au scale uncertainty, which is shown as boxes in the following figures, is the quadrature sum of uncertainties on the p+p cross section of 9.6%, and the number of binary collisions in each centrality bin.

The systematic error on the Au+Au nuclear modification factors is derived by propagating the systematic errors on p+p and Au+Au data [ 5] to the final ratio. The average systematic error for pions is approximately 15%, while for protons and antiprotons it is on the order of 19%. The normalization uncertainty, as in d+Au, is the quadrature sum of uncertainties on the p+p cross section and the number of binary collisions in the corresponding Au+Au centrality bin. For the most central Au+Au bin,  $N_{coll}=1065.4\pm 105.3$ , while for the most peripheral centrality bin,  $N_{coll}=14.5 \pm 4.0$ .

## 3. Results

### 3.1. Proton to Pion Ratio

The proton to pion ratio from minimum bias p+p and minimum bias d+Au are compared to each other and to central and peripheral Au+Au collisions in Figure 1.

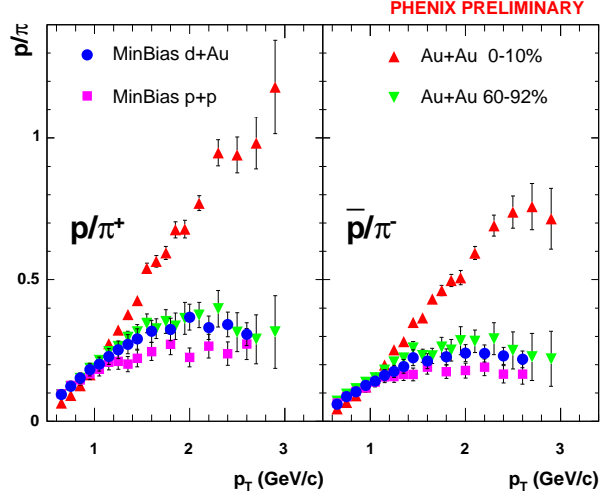


**Fig. 1.** The ratio of protons to  $\pi^+$  and antiprotons to  $\pi^-$  in minimum bias p+p and d+Au compared to peripheral and Au+Au collisions. Statistical error bars are shown.

As noted above, protons and antiprotons are feed-down corrected in each system.

The  $p/\pi$  ratio in d+Au is very similar to that in peripheral Au+Au collisions, and lies slightly above the p+p ratio. The  $p/\pi$  ratio in central Au+Au collisions is, however, much larger. The difference between the ratio in d+Au and central Au+Au clearly indicates that baryon yield enhancement is not simply an effect of sampling a large nucleus in the initial state. The large enhancement requires the presence of a substantial volume of nuclear medium with high energy density.

### 3.2. Nuclear Modification Factors

The measurement of identified hadrons in both d+Au and p+p collisions allows study of the centrality dependence of the nuclear modification factor in d+Au. A standard way to quantify nuclear medium effects on high  $p_T$  particle production in nucleus-nucleus collisions is provided by the *nuclear modification factor*. This is the ratio of the d+A invariant yields to the scaled p+p invariant yields:

$$R_{dA}(p_T) = \frac{(1/N_{dA}^{evt}) d^2 N_{dA}/dydp_T}{T_{dAu} d^2 \sigma_{inel}^{pp}/dydp_T}, \quad (2)$$

where  $T_{dAu} = \langle N_{coll} \rangle / \sigma_{inel}^{pp}$  describes the nuclear geometry, and  $d^2 \sigma_{inel}^{pp}/dydp_T$  for p+p collisions is derived from the measured p+p cross section.  $\langle N_{coll} \rangle$  is the average number of inelastic NN collisions determined from the Glauber simulation described above.

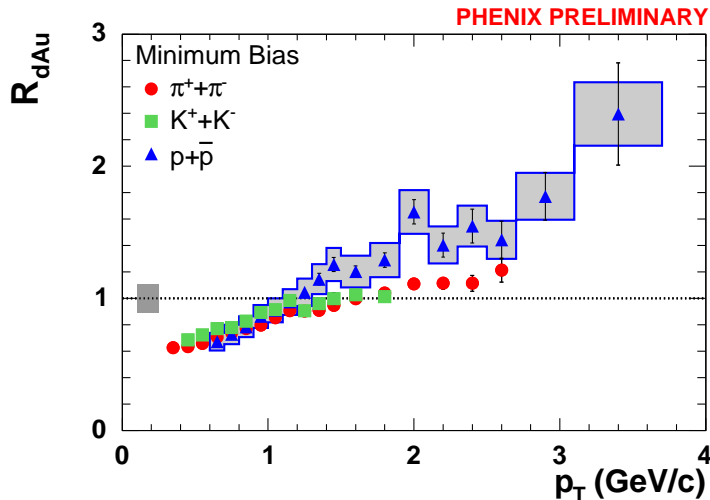


**Fig. 2.** Nuclear modification factor  $R_{dA}$  for pions, kaons and protons in d+Au collisions for Minimum Bias events. The error bars represent the statistical errors, while the systematic errors, which are dominated by uncertainties in the absolute yield and calculation of  $N_{coll}$ , are shown as vertical bars. Point to point errors are also shown for the protons and antiprotons.

Figure 2 shows  $R_{dA}$  for pions, kaons and protons for the minimum bias d+Au centrality bin. We observe a nuclear enhancement in the production of hadrons with  $p_T \geq 1.5 - 2$  GeV/c in d+Au collisions, compared to that in p+p. As was already suggested when comparing the enhancement for inclusive charged hadrons with that of neutral pions [27], there is a species dependence in the Cronin effect. The Cronin effect for charged pions is small, but non-zero, as was observed for neutral pions. The nuclear enhancement for protons and antiprotons is considerably larger, in agreement with [28]. The kaon measurement has a more limited kinematic range, but the  $R_{dA}$  is in agreement with that of the pions at comparable  $p_T$ .

Figure 3 shows  $R_{dA}$  for pions, kaons and protons in the four d+Au centrality bins. Peripheral d+Au collisions, which include an average of 3 nucleon-nucleon collisions, do not show modification of high momentum hadron production, compared to that in p+p collisions. At  $p_T \leq 1$  GeV/c, the nuclear modification factor falls below 1.0. This is to be expected as soft particle production scales with the number of participating nucleons, not with the number of binary nucleon-nucleon collisions. More central collisions show increasing nuclear enhancement in both high  $p_T$  pion and proton production.

The bands in Figure 3 show a calculation of the Cronin effect for pions by Accardi and Gyulassy, using a p-QCD model of multiple semi-hard collisions and taking geometrical shadowing into account [13]. The agreement above 1 GeV/c,

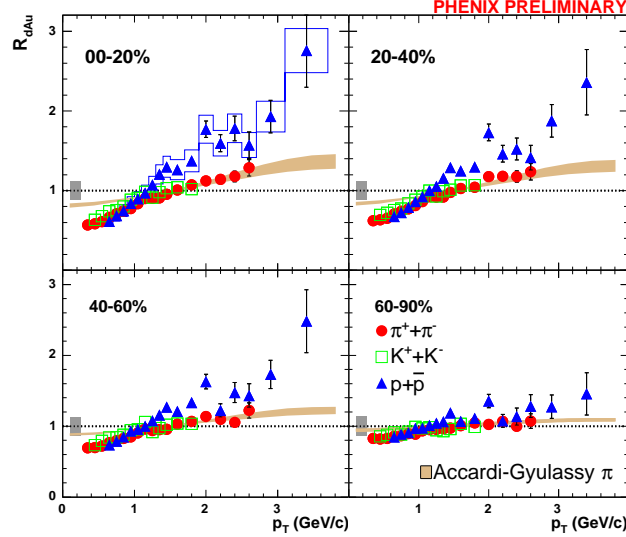


**Fig. 3.** Nuclear modification factor  $R_{dA}$  for pions, kaons and protons in d+Au collisions in four centrality bins. The error bars represent the statistical errors, while the systematic errors, which are dominated by uncertainties in the absolute yield and calculation of  $N_{coll}$ , are shown as vertical bars.  $p_T$  dependence of the systematic uncertainty is minimal and included in the magnitude of the bar. The solid bands show the calculation of the nuclear modification factors for pions by Accardi and Gyulassy [13].

where the calculation should be reliable, is very good for all four centrality bins. The agreement illustrates the effects of multiple partonic scattering and nuclear shadowing. The quantitative agreement leaves very little room for dynamical shadowing effects in the nuclear initial state at mid-rapidity at RHIC.

Figures 4, 5 and 6 compare the nuclear modification factors for pions, kaons and (anti)protons in Au+Au and d+Au collisions. Central and peripheral Au+Au collisions are compared to central d+Au collisions, which have similar number of binary collisions as the peripheral Au+Au sample. Pions show a much lower  $R_{AA}$  at high  $p_T$  in central than in peripheral Au+Au collisions, as expected from the large energy loss suffered by the quarks in central collisions. The nuclear modification factor is slightly larger in d+Au than in peripheral Au+Au, despite the comparable number of binary collisions, but we can not draw a definite conclusion due to the large systematic error of the peripheral  $R_{AA}$ .

The proton and antiproton nuclear modification factors show a quite different trend, however. The Cronin effect, larger than 1.0 at higher  $p_T$  values, is independent of centrality in Au+Au collisions. This feature was already observed as binary collision scaling of proton and antiproton production in the central/peripheral collision yield ratios [4]. The Cronin effect in d+Au is at least as large as in peripheral

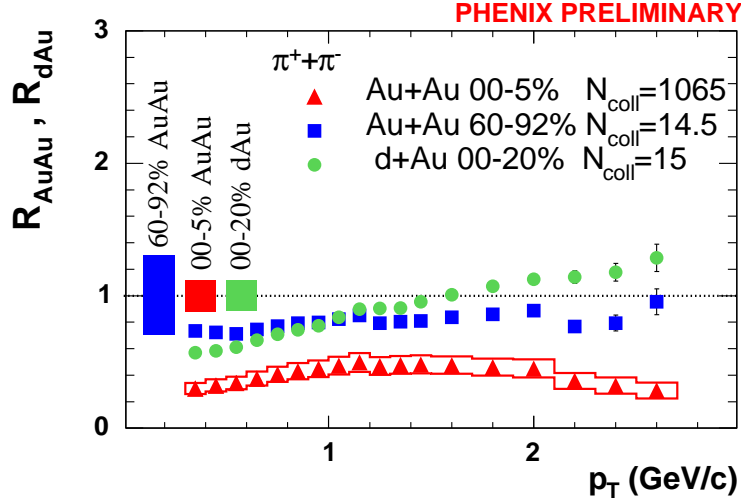


**Fig. 4.** Nuclear modification factors for charged pions, comparing central and peripheral Au+Au collisions to central d+Au. It should be noted that the number of binary nucleon-nucleon collisions in peripheral Au+Au and central d+Au is very similar. Solid bars on the left indicate  $p_T$ -independent normalization uncertainties on the nuclear modification factors for the three systems; error bars indicate statistical errors only.

Au+Au. The difference indicates that baryon production must involve a complex interplay of processes in addition to initial state nucleon-nucleon collisions.

#### 4. Conclusions

Results on identified particle production in p+p, d+Au and Au+Au collisions at  $\sqrt{s_{NN}} = 200$  GeV with the PHENIX spectrometer are presented. The Cronin effect in d+Au collisions for charged pions is small, but non-zero. The proton to pion ratio in d+Au is similar to that in peripheral Au+Au, while the corresponding ratio in p+p is somewhat lower. The nuclear modification factor in d+Au for protons shows a larger Cronin effect than that for pions but is not large enough to account for the abundance of protons in central Au+Au collisions. The difference between pions and protons does, however, indicate that the Cronin effect is not simply multiple scattering of the incoming partons.  $R_{AA}$  for protons and antiprotons confirms previous observations that the production of high  $p_T$  baryons in Au+Au scales with the number of binary nucleon-nucleon collisions.



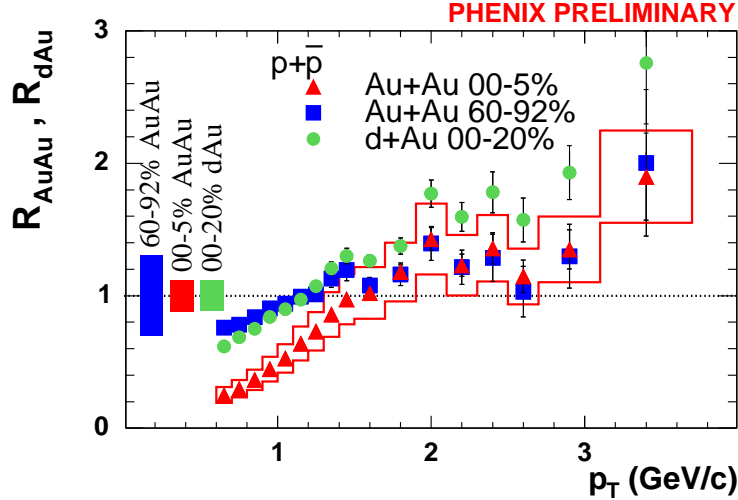


**Fig. 5.** Nuclear modification factors for protons and antiprotons, comparing central and peripheral Au+Au collisions to central d+Au.

## References

1. K. Adcox *et al.* [PHENIX Collaboration], Phys. Rev. Lett. **88**, 022301 (2002).
2. S.S. Adler *et al.* [PHENIX Collaboration], Phys. Rev. Lett. **91**, 072301 (2003).
3. K. Adcox *et al.* [PHENIX Collaboration], Phys. Rev. Lett. **88**, 242301 (2002).
4. S.S. Adler *et al.* [PHENIX Collaboration], Phys. Rev. Lett. **91**, 172301 (2003).
5. S.S. Adler *et al.* [PHENIX Collaboration]. Phys. Rev. **C69**, 034909 (2004).
6. M. Gyulassy and M. Plümer, Phys. Lett. **B243**, 432 (1990); X.N. Wang and M. Gyulassy, Phys. Rev. Lett. **68**, 1480 (1992).
7. R. Baier, D. Schiff and B.G. Zakharov, Annu. Rev. Nucl. Part. Sci. **50**, 37 (2000), and references therein.
8. D. Kharzeev, E. Levin and L. McLerran, Phys. Lett. **B561**, 93 (2003).
9. J.W. Cronin *et al.*, Phys. Rev. **D11**, 3105 (1975).
10. P.B. Straub *et al.* Phys. Rev. Lett. **68**, 452 (1992).
11. D. Antreasyan *et al.*, Phys. Rev. **D19**, 764 (1979).
12. M. Lev and B. Petersson, Z. Phys. **C21**, 155 (1983).
13. A. Accardi and M. Gyulassy, Phys. Lett. **B586**, 244 (2004).
14. G. Papp, P. Levai, G.I. Fai, Phys. Rev. **C61**, 021902 (2000).
15. I. Vitev, M. Gyulassy, Phys. Rev. Lett. **89**, 252301 (2002).
16. X.N. Wang, Phys. Rev. **C61**, 064910 (2000).
17. B.Z. Kopeliovich, J. Nemchik, A. Schaefer and A.V. Tarasov, Phys. Rev. Lett. **88** 232303 (2002).
18. R.C. Hwa and C.B. Yang, Phys. Rev. **C70**, 037901 (2004).

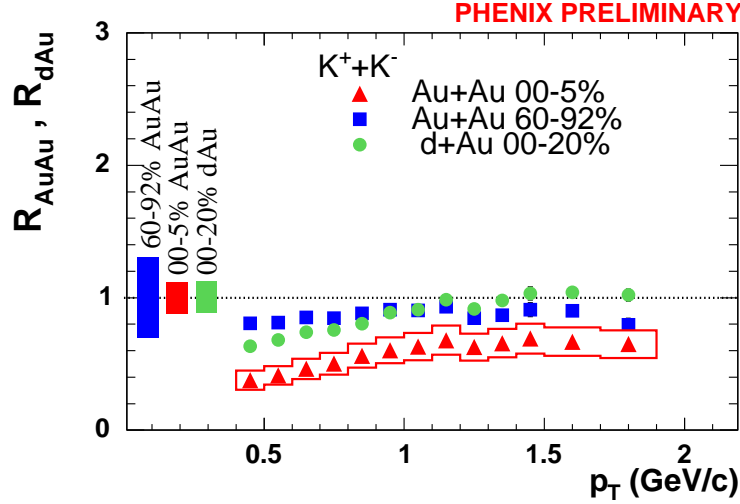


**Fig. 6.** Nuclear modification factors for kaons, comparing central and peripheral Au+Au collisions to central d+Au.

19. K. Adcox *et al.*, Nucl. Instrum. Methods **A499** 469 (2003).
20. R.J. Glauber and G. Matthiae, Nucl. Phys. **B21**, 135 (1970).
21. S.S. Adler *et al.* [PHENIX Collaboration], Phys. Rev. Lett. **94**, 082302 (2005).
22. R.E. Ansorge *et al.* [UA5 Collaboration], Nucl. Phys. **B328**, 36 (1989).
23. J. Adams *et al.*, [STAR Collaboration], nucl-ex/0403020, (2004).
24. M. Heinz *et al.*, [STAR Collaboration], J. Phys. G **31**, S141 (2005)
25. X. Cai [STAR Collaboration], 8th International Conference on Strangeness in Quark Matter, Cape Town, South Africa (2004).
26. R. Witt [STAR Collaboration], nucl-ex/0403021 (2004).
27. S.S. Adler *et al.* [PHENIX Collaboration], Phys. Rev. Lett. **91**, 072303 (2003).
28. J. Adams *et al.* [STAR Collaboration], nucl-ex/0309012 (2003).